2011

Effect of Titanium Dioxide Supports on the Activity of Pt-Ru toward Electrochemical Oxidation of Methanol

Roderick E. Fuentes
University of South Carolina - Columbia

Brenda L. García
University of South Carolina - Columbia

John W. Weidner
University of South Carolina - Columbia, weidner@engr.sc.edu

Publication Info

Journal of the Electrochemical Society, 2011, pages B461-B466.

Publisher's link: http://dx.doi.org/10.1149/1.3559495
DOI: 10.1149/1.3559495

Journal of The Electrochemical Society, **158** (5) B461-B466 (2011)
0013-4651/2011/158(5)/B461/6/$28.00 © The Electrochemical Society

Effect of Titanium Dioxide Supports on the Activity of Pt-Ru toward Electrochemical Oxidation of Methanol

Roderick E. Fuentes,[*] Brenda L. García,[,a] and John W. Weidner[***,z]**

Department of Chemical Engineering, University of South Carolina, Columbia, South Carolina 29208, USA

TiO_2 and Nb-TiO_2 were investigated as stable supports for Pt-Ru electrocatalysts towards methanol oxidation. X-ray photo-electron spectroscopy (XPS) data for all these TiO_2-based supports show oxidation states of Ti^{4+}, with no Ti^{3+}, suggesting low electronic conductivity. However, the deposition of metal nanoparticles onto the supports at loadings of 60 wt% metal dramatically increased conductivity, making these electrodes (metal particles + support) suitable for electrochemistry even though the supports have low conductivity. For some of these TiO_2-based supports, the activity of Pt-Ru towards methanol oxidation was excellent, even surpassing the activity of the same electrocatalysts supported on carbon. The activity of the electrocatalyst depended on TiO_2 crystalline structure, the addition of Nb into the support and the weight loading of metal. For example, using anatase Nb-TiO_2 as a support increased the electrochemical activity of Pt-Ru by 83% compared to the same electrocatalysts supported on either carbon Vulcan XC-72R or rutile Nb-TiO_2. This electrode was also 64% more active than the one that had anatase TiO_2 as the support with no Nb. Finally, increasing the weight loading of metal from 5 to 60% increased the conductivity by 5 orders of magnitude and the activity by a factor of 20.
 [DOI: 10.1149/1.3559495]

Manuscript submitted June 1, 2010; revised manuscript received January 24, 2011. Published March 10, 2011.

Electrodes require an electrically conductive material to provide a conductive path for the electrons to travel from the reaction site to the current collector. Often, the electrocatalyst serves the dual purpose of facilitating the electrochemical reaction and transporting the electrons. However, when the electrocatalyst is a precious metal such as platinum, it is advantageous to support it on a conductive substrate such as carbon. This enables the expensive electrocatalyst to be highly dispersed, thus minimizing the amount of precious metal without sacrificing catalytic activity. Dispersion of precious metals onto inexpensive supports is the same approach used in heterogeneous catalysts for non-electrochemical reactions. In these cases though, the support is often an insulating metal-oxide material that has high surface area and promotes catalytic activity (i.e., enhanced catalyst-support interactions). In electrochemical applications (e.g., proton exchange membrane fuel cells), the typical support material is carbon due to its high surface area and high electron conductivity rather than any enhanced catalyst-support interactions. However, carbon-supported electrodes that operate at voltages above ~0.9 V in the presence of water are known to undergo carbon corrosion.[1] Corrosion of the support can create a loss of electrical contact with the catalyst particle, thus decreasing the performance of the cell.

Replacing carbon with traditional metal-oxide supports is usually not considered due to their electrical-insulating properties at temperatures below 200°C. Instead, attempts have been made to impart electrical conductivity to metal oxides. For example, reduced oxidation state titania (e.g., Ti_4O_7 and Ebonex) and niobium-doped TiO_2 have shown promise for electrically conductive supports.[2–5] Titanium oxide based supports may also provide catalytic advantages for some electrochemical reactions (e.g., oxidation of methanol). This may be especially true for the anatase crystal structure of TiO_2 since it is a more active catalyst for oxidizing organic compounds compared to the rutile and brookite structures.[6–8] Morris et al.[9] studied mixtures of NbO_2 and TiO_2 sintered at high temperatures to form $Nb_{0.1}Ti_{0.9}O_2$, but the material becomes the more stable and less catalytically active rutile structure. Chen et al.[3] and Huang et al.[4] synthesized a rutile form of Nb-TiO_2 and measured conductivity on the order of 1 S/cm and a surface area about 2 m^2/g. Unfortunately, this is a relatively low surface area. Also a conductive form of anatase Nb-TiO_2 has not been reported. To preserve an anatase crystalline structure, temperatures below 800°C needs to be maintained.[10]

Therefore, we synthesized the anatase form of Nb-TiO_2 by modifying a low temperature surfactant-templating method developed by Yan et al.[11] for pure TiO_2.[12] Our high surface area support material (132 m^2/g) was fabricated into membrane electrode assemblies (MEAs) and showed activity towards the electrochemical oxidation of methanol in a fuel-cell environment. This is consistent with recent results published by Gojkovic et al.[5] that reported electrochemical activity of Pt and Pt-Ru on anatase Nb-TiO_2. However, it was unclear if a conductive support was produced via a low temperature synthesis route. In this paper, the synthesis method for anatase and rutile Nb-TiO_2 supports were refined based on the method by Cassiers et al.[13] A colloidal procedure to distribute platinum-ruthenium bimetallic nanoparticles onto these supports and commercial forms of pure anatase and rutile TiO_2 was developed from the work of Bock et al.[14] These electrode materials were then fully characterized using X-ray Diffraction (XRD), X-ray Photoelectron Spectroscopy (XPS), Brunauer-Emmett-Teller (BET) surface area, Scanning Microscope Electrode with Energy dispersive X-ray Spectroscopy (SEM-EDX), Atomic Absorption (AA) spectrometry, High Resolution Transmission Electron Microscopy (HRTEM), electronic conductivity tests and O_2-H_2 titration to measure Pt surface area in a chemisorption system. Finally, the activity of the Pt-Ru nanoparticles supported on anatase and rutile forms of both Nb-TiO_2 and pure TiO_2 were measured for methanol oxidation using cyclic voltammetry and compared to the activity of Pt-Ru nanopoarticles supported on carbon Vulcan XC-72R.

Experimental

Titanium Oxide Supports.—Niobium addition into titanium dioxide was adapted from the procedure to synthesize TiO_2 of Cassiers et al.[13] The complex NbTi-CTABr was synthesized by adding 0.1125 mol of titanium (IV) butoxide (Sigma-Aldrich) and 0.0125 mol of niobium (V) ethoxide (Sigma-Aldrich) to a solution containing hydrochloric acid and ethanol. The relative amounts of Nb:Ti was chosen to produce a material with the stoichiometry 0.1:0.9 (i.e., $Nb_{0.1}Ti_{0.9}O_2$). This material will be referred as Nb-TiO_2 throughout the paper. This solution was stirred until the precursors were dissolved. An ethanolic solution of 0.02 mol of cetyltrimethylammonium bromide (CTABr) (Sigma-Aldrich) was added and the complex was formed in a Petri dish for several days at a temperature of 60°C. A solution of de-ionized (DI) water with ammonium hydroxide (NH_4OH) was prepared with a *p*H of 9–10. The resulting solid was transferred to the solution of DI water and NH_4OH in continuous stirring and kept for 48 h. During this time the *p*H was maintained between 9 and 10 using NH_4OH. To obtain the Nb-TiO_2 with

[*] Electrochemical Society Student Member.
[**] Electrochemical Society Active Member.
[***] Electrochemical Society Fellow.
[a] Present address: Center for Hydrogen Research, Savannah River National Lab, Aiken, SC.
[z] E-mail: weidner@engr.sc.edu

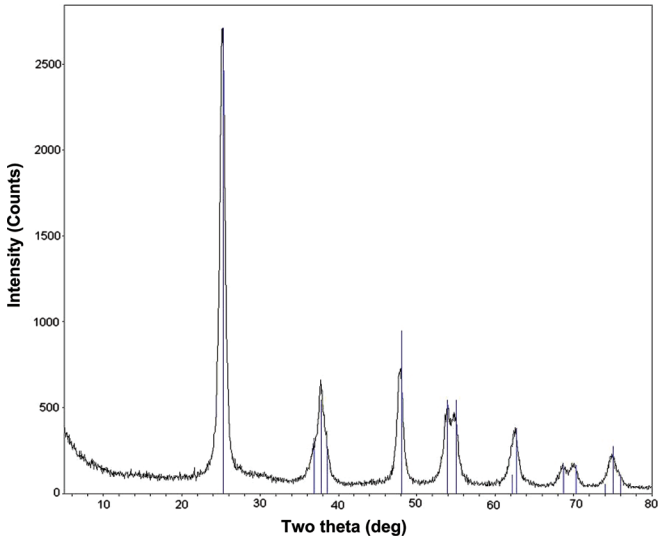

Figure 1. (Color online) X-Ray Diffraction data for Nb-TiO_2. The vertical lines represent the guidelines for anatase TiO_2.

an anatase crystalline structure, the sample was calcined at 400°C for 2 h. The sample was further calcined at 1000°C for 2 h to convert the structure from anatase to rutile. The resulting anatase or rutile powder was crushed into a fine powder with a pestle and mortar. For comparison, pure TiO_2 with anatase structure and pure TiO_2 with rutile structure were purchased from Sigma-Aldrich.

Deposition of 1:1 Pt:Ru Bimetallic Nanoparticles onto Supports.—Platinum-ruthenium nanoparticles were deposited onto the supports using an ethylene-glycol procedure published by Bock et al.[14] A solution of 0.2 M sodium hydroxide in ethylene glycol (150 mL) was added to a round bottom flask, and 400 mg of the support (Nb-TiO_2, TiO_2 or carbon Vulcan XC-72R) was added. The sample was sonicated to disperse the particles in solution. Under a nitrogen environment, 2.03 mmol of ruthenium (III) chloride (Sigma-Aldrich) and 2.03 mmol of platinum (IV) chloride (Sigma-Aldrich) were added to the mixture, allowed to mix for 2 h, and subsequently heated to 160°C for 3 h. The sample was mixed with approximately 1000 mL of DI water and nitric acid was added until the *p*H reached 1.0. The colloidal suspension was mixed for 3 h. After allowing the solution

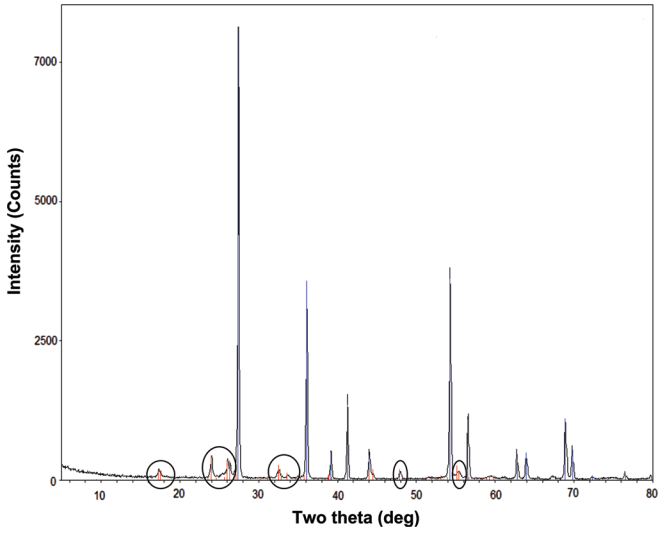

Figure 2. (Color online) X-Ray Diffraction data for Nb-TiO_2. The vertical lines represent the guidelines for rutile TiO_2. The peaks in circles represent the guidelines for titanium niobium oxide ($TiNb_2O_7$).

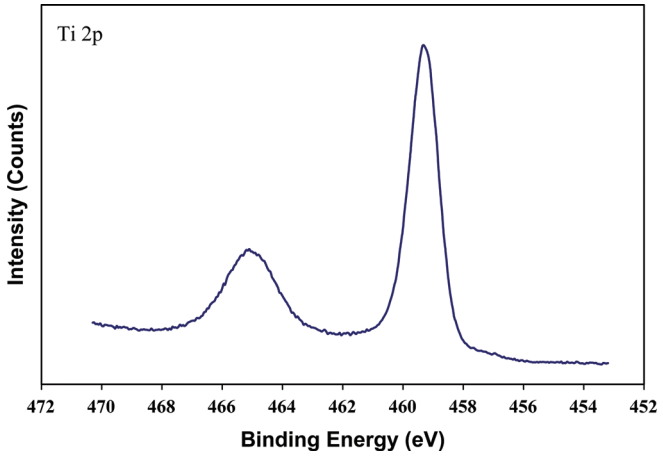

Figure 3. (Color online) Ti 2p core-level XPS spectrum of Nb-TiO_2.

to settle for 5 h, the sample was filtered and washed with several aliquots of water. The sample was dried at 110°C for 4 h under vacuum conditions. The resulting material was crushed with a pestle and mortar to obtain a fine powder.

Materials Characterization.—XRD was performed on a Rigaku 405S5 to examine the crystal structure of the oxide support materials. XRD patterns were compared with reference spectra using the software JADE (Materials Data, Inc.). XPS studies were obtained using Kratos Hsi monochromatized XPS with ultraviolet photoelectron spectroscopy (UPS) source. Elemental Analysis in a Scanning Microscope Electrode with Energy dispersive X-ray Spectroscopy (SEM-EDX) in a Quanta 200 FEI confirmed a 1:1 ratio of Pt to Ru. Weight percentages of the samples were confirmed by analyzing a solution of catalyst dissolved via acid digestion using PerkinElmer Atomic Absorption (AA) spectrometers. HRTEM images were obtained on a JEOL 2100 F TEM with accelerating voltage of 80–200 kV. BET surface areas measurements were recorded using a Nova 2000 high speed gas adsorption analyzer. The samples were dried at 300°C for 3 h under vacuum prior to analysis. The surface areas were obtained using liquid nitrogen temperature (77 K) and a six point BET was used for calculating the specific surface area. The experiments were replicated with a new sample from the same batch of material and the average of the two runs is reported here. The adsorbate used was nitrogen gas.

Electronic conductivity was measured on pressed pellets using a 13 mm diameter die set from International Crystal Laboratories. For making the pellets, 0.6 g of material were added inside the die. The assembly was pressed to approximately 2 metric tons using a Carver

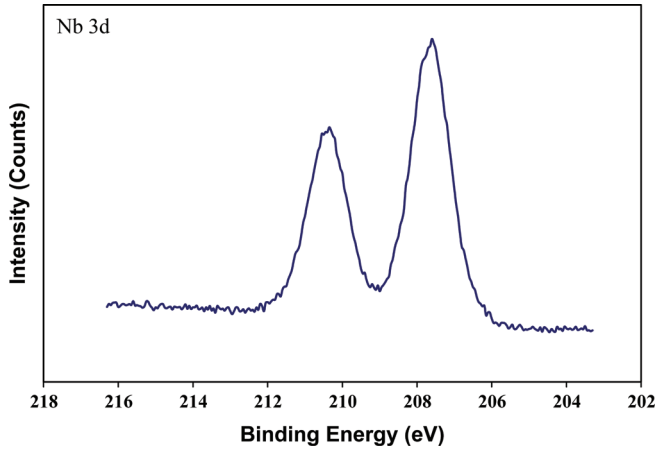

Figure 4. (Color online) Nb 3d core-level XPS spectrum of Nb-TiO_2.

Table I. Surface areas of the Nb-TiO_2 materials synthesized here as well as commercial TiO_2 and carbon Vulcan XC-72R materials.

Sample	BET Surface Area (m^2/g)
Nb-TiO_2 anatase	194
Nb-TiO_2 rutile	5
TiO_2 anatase	170
TiO_2 rutile	213
Carbon Vulcan XC-72R	232

hydraulic press. Gold wires were attached at opposite sides of the pellet with silver conductive epoxy (Ted Pella, Inc.). The test was performed connecting the pellet using a two point measurement in a Princeton Applied Research VMP3 potentiostat. Electrochemical impedance ran from a frequency of 200 W to 10 kW using EC-Lab software.

The surface areas of platinum for the bimetallic Pt-Ru nanoparticles were obtained using hydrogen titration of adsorbed oxygen in a chemisorption setup (AutoChem II 2920 from Micromeritics) using a procedure described previously.[15] This procedure takes advantage of the fact that adsorbed oxygen can be titrated from Pt at low temperatures (<100°C), while significantly higher temperatures are required for Ru. The average surface areas and standard deviations are reported here based on 3–4 replicated measurements. The platinum dispersion was obtained from the software of the chemisorption and is defined as the fraction of platinum atoms on the surface of the nanoparticles.

The cyclic voltametry experiments consisted of a 5 mm diameter glassy carbon disc working electrode, a luggin capillary $Hg/HgSO_4$ reference electrode and a Pt wire as the counter electrode. The CorrWare software was used to record the data. The experiments were run at room temperature in a scan window of −0.02 to 1.28 V versus SHE with a cyclic sweep rate of 50 mV/s for 35 cycles, and then three cycles were recorded at 5 mV/s. A solution of 0.5 M H_2SO_4 and 1 M methanol was used as the electrolyte. The ink used for the electrode film consisted of 6 mg of the electrode material sonicated with 3 mL of DI water and 3 mL of isopropyl alcohol (IPA). A volume of 18.5 μL was placed on the electrode. The sample was binded

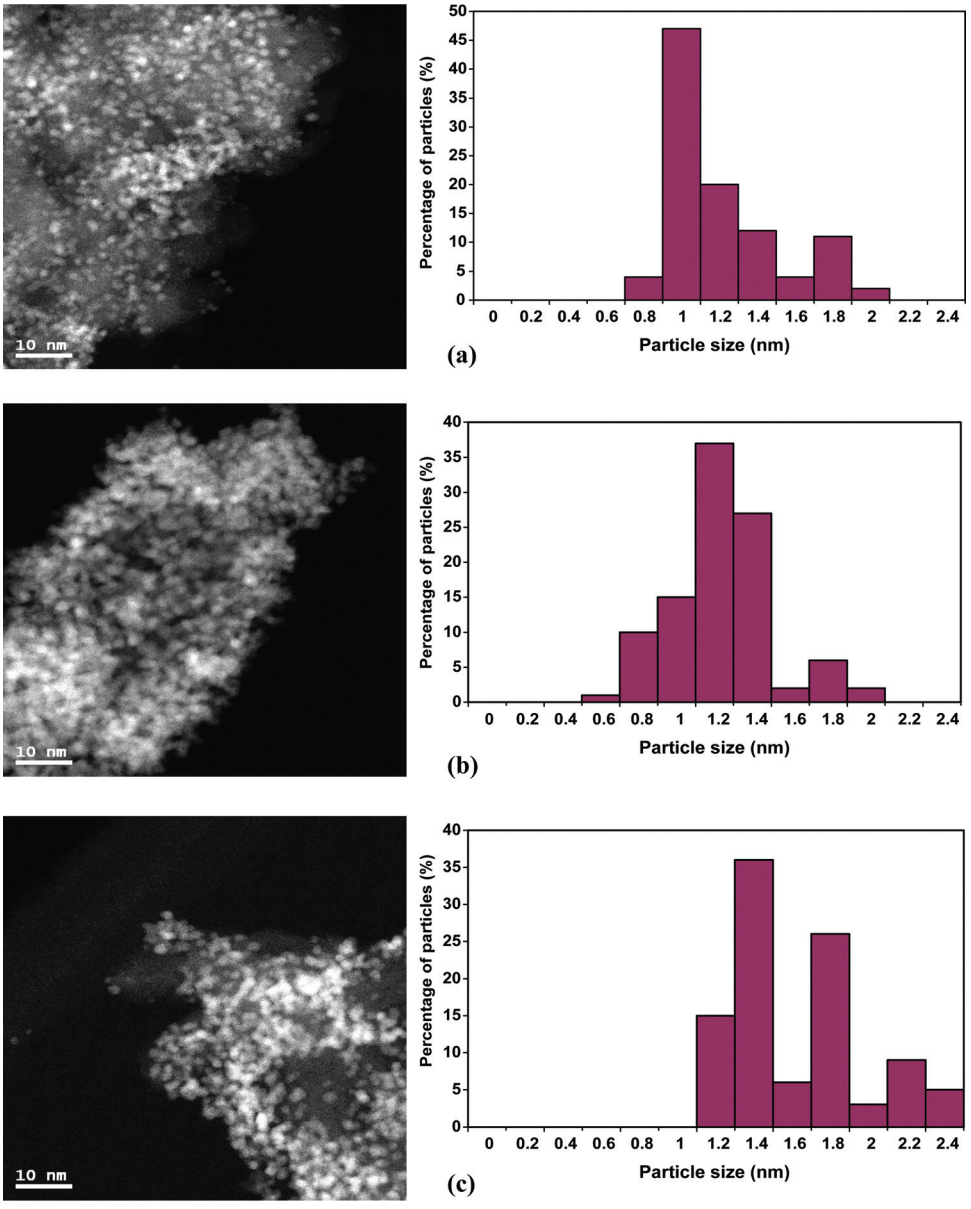

Figure 5. (Color online) HRTEM images and histograms of 60 wt% Pt-Ru on: (a) anatase Nb-TiO_2; (b) anatase TiO_2; and (c) rutile TiO_2.

with a solution of 5 wt% nafion:IPA (1:20 ratio). All the voltammograms presented here are the third and final scan normalized by the surface area of platinum on the electrode.

Results and Discussion

The crystalline structure for the anatase and rutile forms of Nb-TiO_2 was verified using XRD, and they are presented in Figs. 1 and 2, respectively. In Fig. 1, the peaks match the structure for anatase TiO_2 structure. No other crystalline phases were detected in the sample, including distinct niobium oxides structures. Since Nb and Ti atom have similar atomic radius and only 10 mol % of Nb is added, a possible explanation is that niobium substitutionally replaces some Ti sites in the lattice of TiO_2 structure. For the synthesis of pure TiO_2 by Cassiers et al.[13] the crystal phases obtained were a mixture of anatase and rutile. This suggests that the addition of niobium into the synthesis procedure may help to preserve the anatase structure. The anatase form of Nb-TiO_2 was heated to 1000°C to obtain the rutile structure.[10] Figure 2 confirms the conversion since the peaks match the structure for rutile TiO_2. Additionally, the spectrum reveals small peaks (identified with a circle) representing titanium niobium oxide ($TiNb_2O_7$) that are usually seen in samples treated at high temperatures.[16]

XPS was used to obtain the oxidation states and the valence-band spectra at the conduction band of our materials. The spectra for anatase Nb-TiO_2 is presented in Figs. 3 and 4. The spectra were scaled using the O 1s peak (not presented) to account for the shifts in the pattern. In Fig. 3, the spectrum shows a doublet peak of Nb $3d_{1/2}$ centered at 207.7 eV and Nb $3d_{4/5}$ centered at 210.4 eV. This corresponds to the molecule Nb_2O_5, which has an oxidation state of Nb^{5+}. Figure 4 shows the Ti 2p peaks. The high intensity peak is Ti $2p_{3/2}$, with a binding energy of 459.3 eV. This has been assigned to TiO_2 with an oxidation state of 4+. In the literature, it is found that Nb^{5+} inserted into titanium dioxide will either create one vacancy of Ti atom per four Nb atoms introduced or reduce an atom of Ti^{4+} to Ti^{3+} per Nb atom introduced.[17] The latter would impart conductivity to the material.[17–20] However, no characteristic Ti^{3+} was observed, as there is not a peak close to the high intensity peak of Ti 2p with less binding energy. A non-conductive oxide material is also consistent with the white color of the samples. Therefore, it is believed that the insertion of Nb^{5+} species created vacancies of Ti atoms to compensate for the excess in charge, instead of a reducing the oxidation state from Ti^{4+} to Ti^{3+}. For Nb-TiO_2 in its rutile form, XPS spectra were also acquired and similar spectra presented for Nb-TiO_2 in its anatase form were obtained. XRD and XPS spectra were also collected for the commercial TiO_2 rutile and TiO_2 anatase powders and similar results to those shown in Figs. 1–4 were obtained.

BET surface area measurements were performed to obtain the surface area of the supports (Table I). For anatase Nb-TiO_2, the surface area measured was 194 m^2/g. This surface area is about 16% lower than the 232 m^2/g value for carbon Vulcan XC-72R, the typical support of commercial fuel cells catalysts, and 62% lower than the 613 m^2/g value for pure TiO_2 reported by Cassiers et al.[13] For the rutile form, prepared by heat treating the Nb-TiO_2 to 1000°C, the surface area was reduced to 5 m^2/g. Anatase and rutile TiO_2 surface areas were also measured by the BET method and the results are presented in Table I. The surface area for anatase Nb-TiO_2 (194 m^2/g) is 14% higher than anatase TiO_2 (170 m^2/g). The commercial rutile TiO_2 had the highest surface of all the TiO_2-based materials at 213 m^2/g. The BET surface areas of the replicas had less than 8% of difference.

Platinum-ruthenium bimetallic nanoparticles were supported on the materials mentioned above and the resulting particle size distributions for these particles were obtained from HRTEM images. An example of the images obtained for Pt-Ru electrocatalyst supported on different materials are shown in Fig. 5. In the images, the bright regions are the metal nanoparticles of platinum-ruthenium, and the gray areas are: (a) anatase Nb-TiO_2; (b), anatase TiO_2 and (c) rutile TiO_2. Generally, at this high loading, the particles seem well dispersed on all three supports. Average particle sizes were determined using a volume distribution and a histogram is presented in Fig. 5 next to HRTEM images. Around 100 particles were analyzed for each material and the average particle size determined for 60 wt% Pt-Ru on: (a) anatase Nb-TiO_2 was 1.37 nm ± 0.29; (b) anatase TiO_2 was 1.36 ± 0.29; and (c) rutile TiO_2 was 1.77 ± 0.34. In Fig. 6, HRTEM images of the anatase and rutile TiO_2 supports are shown (i.e., not catalyst particles). It is observed that anatase TiO_2 particles are round in shape with a diameter in the 10 to 20 nm range. The particles on rutile TiO_2 have an elongated elliptical shape with higher diameters than anatase TiO_2. The average particle size of 60% Pt-Ru/ TiO_2 rutile is increased by 30% compared to the average particle sizes of the other two materials from Fig. 5. As seen on the HRTEM image for this catalyst (Fig. 5), the metal particles tends to agglomerate more in specific areas, leaving void space on the support.

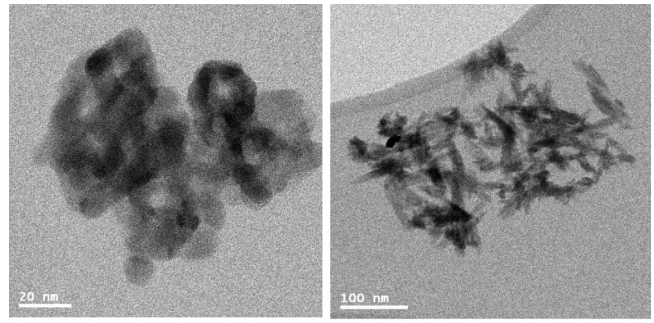

Figure 6. HRTEM images of: (a) anatase TiO_2; and (b) rutile TiO_2 supports only.

Based on the XPS data, the support is not electronically conductive. However, previous data has shown that methanol oxidation can occur on MEAs made from Pt-Ru electrocatalysts supported on Nb-TiO_2.[12] To determine if the metal electrocatalyst could impart sufficiently conductivity to the electrode, the electronic conductivity of the electrode was measured as a function of weight percent platinum loading (see Fig. 7). At low platinum loadings (<10%), the conductivity of the electrode is on the order of 10^{-5} S/cm. Increasing the weight percent of the metal increases the conductivity by orders of magnitude. For example, at 60% Pt loading the conductivity of 1.26 S/cm was measured, 10^5 orders of magnitude increase over that of the support. Therefore, it appears that increasing the amount of metal on the support increases the electronic conductivity

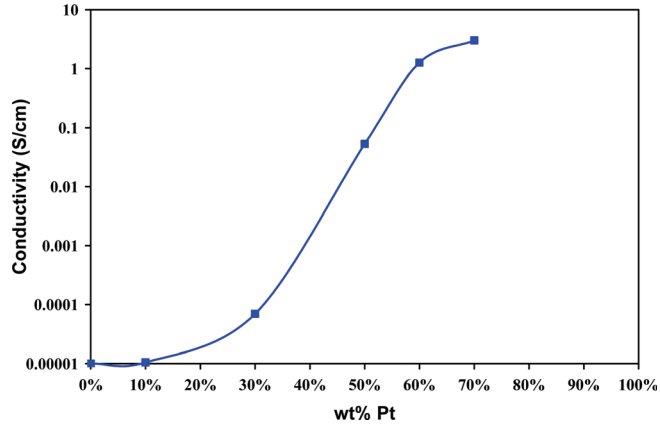

Figure 7. (Color online) Electronic conductivity of anatase Nb-TiO_2 at room temperature as a function of weight percent loading of platinum.

Table II. Platinum surface areas and platinum dispersions of the electrocatalysts measured by chemisorption. The first three samples shown above are on average of three measurements, and the values from the last fours are on average of four measurements.

Sample	Pt Surface Area (m^2/g of Pt)	Pt Dispersion (%)
60 wt% Pt-Ru/TiO_2 anatase	55.8 ± 0.97	22.4
60 wt% Pt-Ru/TiO_2 rutile	54.5 ± 2.5	22.1
60 wt% Pt-Ru/Nb-TiO_2 rutile	14.5 ± 1.1	5.88
60 wt% Pt-Ru/Nb-TiO_2 anatase	33.9 ± 1.1	13.7
40 wt% Pt-Ru/Nb-TiO_2 anatase	32.6 ± 1.0	13.2
5 wt% Pt-Ru/Nb-TiO_2 anatase	88.8 ± 4.9	35.9
60 wt% Pt-Ru/Carbon Vulcan XC-72R	53.1 ± 1.2	21.5

of the electrode (metal particles + support) to levels that can sustain an electrochemical reaction.

Table II gives the average and the standard deviation of the platinum surface area and the average platinum dispersion for each of the electrocatalysts using chemisorption. For 60 wt% Pt-Ru supported on anatase TiO_2, rutile TiO_2 and carbon Vulcan XC-72R, the platinum surface area and platinum dispersion of the catalyst particles are all approximately 54 m^2/g and 22%, respectively, even though there is a slight variation in BET surface areas of the support (see Table I). However, the 60 wt% Pt-Ru on anatase Nb-TiO_2 platinum surface area is approximately 36% smaller at 34 m^2/g (14% Pt dispersion) despite the comparable BET surface areas of the supports. The Pt surface area for 60 wt% Pt-Ru on rutile Nb-TiO_2 is only 14.5 m^2/g (5.9% Pt dispersion), which is more than a factor of 2 smaller than that catalyst on anatase Nb-TiO_2. This correlates to the low BET surface area, which is 39 times smaller. The surface area of the support does seem to play a role in the utilization of the catalysts deposited on it, but the relationship is not linear. Another factor affecting catalyst utilization is the percent loading of the metal. Lowering the loading of Pt-Ru from 60 to 40 wt% has a negligible effect in the platinum surface area, but further lowering to 5 wt% Pt-Ru increases the Pt surface area from 33.9 to 88.8 m^2/g (a 2.6 fold increase) and the Pt disperson from 13.7 to 35.9%.

To measure the electrocatalytic activity of the various electrode materials, CV experiments for methanol oxidation were performed and the results are presented in Figs. 8–10. The currents in these figures are normalized with respect to the active surface area of platinum on the electrode (see Table II). In the CVs, the small currents around 0 V correspond to hydrogen oxidation/reduction. As the potential is increased in the positive direction, a peak at approximately 0.9 V indicates the oxidation of methanol and at a voltage of more than 1.2 V, water electrolysis occurs. Upon reversing the scan, an additional methanol oxidation peak at approximately 0.7 V is observed. The normalized peak current during the forward scan at 0.9 V is defined here as the activity of the electrocatalyst towards methanol oxidation.

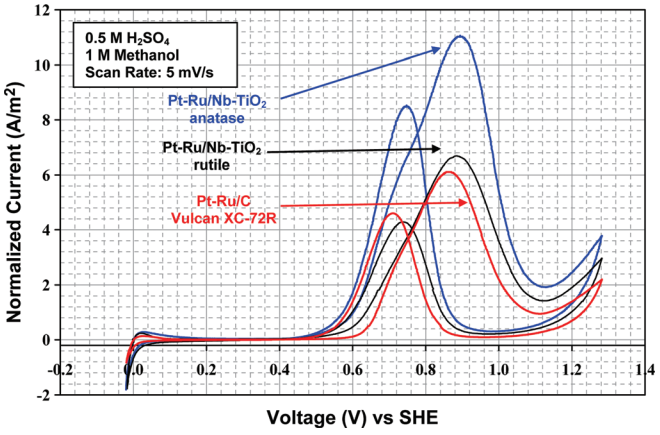

Figure 8. (Color online) Cyclic voltammograms of Pt-Ru catalysts supported on carbon Vulcan XC-72R and two different crystal structures of Nb-TiO_2. The loading of platinum and ruthenium is 60 wt%. The currents are normalized by the platinum activity surface area.

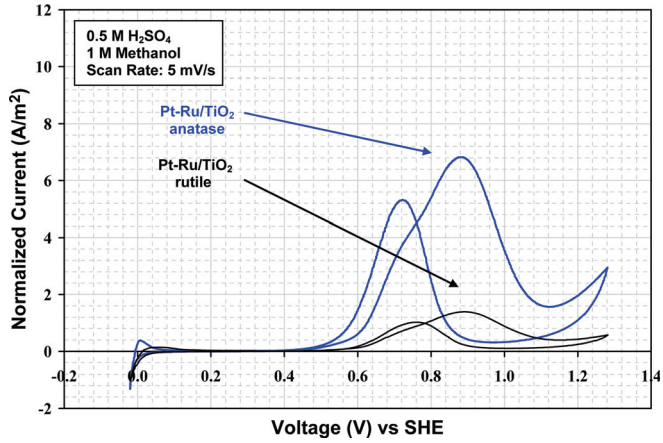

Figure 9. (Color online) Cyclic voltammograms of Pt-Ru catalysts supported on anatase and rutile TiO_2. The loading of platinum and ruthenium is 60 wt%. The currents are normalized by the platinum activity surface area.

Figure 8 shows the cyclic voltammogram for 60 wt% Pt-Ru on anatase Nb-TiO_2, rutile Nb-TiO_2 and carbon Vulcan XC-72R. It is observed that Pt-Ru/Nb-TiO_2 anatase has the highest activity. Comparing Pt-Ru on anatase Nb-TiO_2 with that on carbon, the former resulted in 83% higher activity. Depositing Pt-Ru on the rutile form of this support had a negligible increase in activity over Pt-Ru/C. Figure 9 shows a comparison of the activity of Pt-Ru towards methanol oxidation for the two different TiO_2 crystal structures obtained commercially (i.e., no Nb). The catalyst deposited on the anatase form of TiO_2 gave almost four times higher activity compared to the same catalyst on rutile TiO_2, consistent with the trends shown in Fig. 8. Therefore, the anatase form of TiO_2 offers a significant enhancement to the activity of the metal catalysts towards methanol oxidation compared to either the rutile form or carbon.

To see if Nb incorporation into the crystal structure of the TiO_2 plays a role in the catalytic activity of the electrode, methanol oxidation CVs in Figs. 8 and 9 are compared. It is observed that Pt-Ru supported on anatase or rutile Nb-TiO_2 have higher activities than Pt-Ru on anatase or rutile TiO_2 (i.e., no Nb). For example, 60 wt% Pt-Ru/Nb-TiO_2 anatase has 64% higher activity than similar Pt-Ru loading on anatase TiO_2. Comparing the rutile forms, the electrode made from the support containing Nb has five times higher activity. The additional factor, however, when comparing the two rutile-based electrodes is that BET surface area of rutile TiO_2 is 43 times higher than rutile Nb-TiO_2. It is possible that the preparation method rather than the existence of Nb may be the reason for the observed activity differences.

To see if overall electrode conductivity correlates with electrochemical activity, a series of methanol oxidation CVs were collected on anatase Nb-TiO_2 with different levels of metal loadings (i.e., 60, 40 and 5 wt% Pt-Ru). In Fig. 10, the same volume (and hence the same total mass) of each material was deposited onto the surface of the disk. This resulted in all three electrodes having the same electrode thickness but different amounts of metal catalysts. However, normalizing the currents by the active area adjusts for the difference in metal loading. Increasing the loading from 40 to 60 wt% increased the activity by 160% while the conductivity increased by 3 orders of magnitude (see Fig. 7). Increasing the loading from 5 to 60 wt% increased the activity by a factor of 10 while the conductivity increased by five orders of magnitude. It is not clear why the

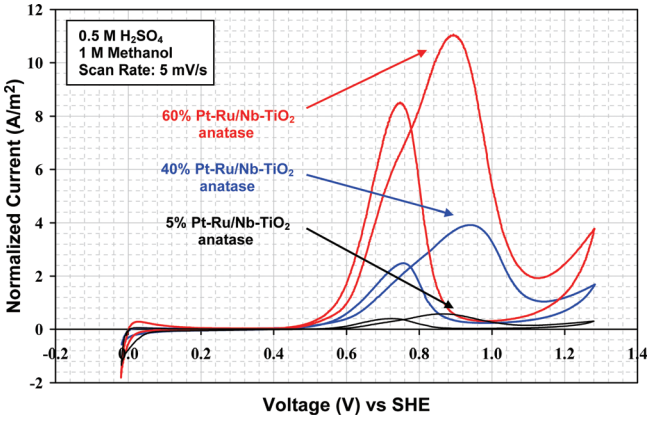

Figure 10. (Color online) Cyclic voltammograms of Pt-Ru catalysts supported on anatase Nb-TiO_2 with different percent loadings of metal. The currents are normalized by the platinum activity surface area.

conductivity should affect the activity so dramatically, or if that indeed is the reason for this difference. It is surprising though that the electrode with only 5% meal could support any electrochemistry considering the extremely low electronic conductivity. Regardless, it is highly unlikely that an electrode with a 5 wt% metal loading would function in a membrane electrode assemble (MEA), where the electrode layer could be two orders of magnitude thicker and the current densities three orders of magnitude higher.

Conclusion

TiO_2 and Nb-TiO_2 were investigated as a stable supports for electrocatalysts. Platinum-ruthenium bimetallic nanoparticles were supported on Nb-TiO_2 and commercial TiO_2 with different crystalline structures and tested for methanol oxidation. X-ray Photoelectron Spectroscopy (XPS) data for all titanium dioxide supports show oxidation states of Ti^{4+}, with no Ti^{3+}, suggestion low electronic conductivity. The addition of niobium during synthesis stabilized the anatase form of TiO_2, but it did not affect the conductivity of the support. Electron conductivity measurements on pressed pellets confirmed low electronic conductivity. However, the loading of metal catalysts particles onto the supports dramatically increased electronic conductivity of the electrode (metal particles + support).

A BET surface area analysis for our synthesized anatase Nb-TiO_2 gave a value of 194 m^2/g, which is about 16% lower than carbon Vulcan XC-72R but 14% higher than pure anatase TiO_2 obtained commercially. The pure rutile TiO_2 had a surface area of 273 m^2/g, where our synthesized rutile Nb-TiO_2 had a very low surface area of 5 m^2/g due to the heat-treatment at 1000°C. Particle size distribution from HRTEM images showed small particle sizes well distributed on all the supports. The average particle sizes were less than 2 nm and the distribution was better in anatase than in rutile.

A series of cyclic voltammograms shows that titanium dioxide crystalline structure, the addition of Nb and weight loading of metal have a significant effect on the activity of the electrodes towards methanol oxidation. For example, using anatase Nb-TiO_2 as a support increased the electrochemical activity by a factor of five compared to the same electrocatalyst supported on rutile Nb-TiO_2. In addition, this electrode was 83 and 64% more active than the one that had Vulcan XC-72R and anatase TiO_2 as the support (i.e., no Nb), respectively. Finally, increasing the weight loading of metal from 5 to 60% increased the conductivity by five orders of magnitude and the activity by a factor of 20. Therefore, as long as the metal loading is high enough, the activity of the electrode towards the methanol oxidation reaction can be improved by using anatase TiO_2 as supports for electrocatalyst. Since these materials are inherently stable, electrodes made from them also should be more durable than those made from carbon.

Acknowledgment

This work was supported by the 2008 E.ON International Research Initiative entitled "Application of Nanotechnology in the Energy Business." The authors would also like to thank Dr. John R. Monnier for his help with the chemisorption measurements.

University of South Carolina assisted in meeting the publication costs of this article.

References

1. L. M. Roen, C. H. Paik and T. D. Jarvi, *Electrochem. Solid-State Lett.*, **7**, A19 (2004).
2. T. Ioroi, Z. Siroma, N. Fujiwara, S. Yamazaki, and K. Yasuda, *Electrochem. Commun.*, **7**, 183 (2005).
3. G. Y. Chen, S. R. Bare, and T. E. Mallouk, *J. Electrochem. Soc.*, **149**, A1092 (2002).
4. S. Y. Huang, P. Ganesan, and B. N. Popov, *Appl. Catal., B.*, **96**, 224 (2010).
5. S. Lj. Gojkovik, B. M. Babic, V. R. Radmilovic, and N. V. Krstajic, *J. Electroanal. Chem.*, **639**, 161 (2010).
6. U. Diebold, *Surf. Sci. Rep.*, **48**, 53 (2003).
7. Y. Sakatani, D. Grosso, L. Nicole, C. Boissiere, G. J. de A. A. Soler-Illia and C. Sanchez,. *J. Mater. Chem.*,**16**, 77 (2006).
8. K.I Hadjiivanov and D. G. Klissurski, *Chem. Soc. Rev.,* **25**, 61 (1996).
9. D. Morris, Y. Dou, J. Rebane, C. E. J. Mitchell and R. G. Egdell, *Phys. Rev. B*, **61**, 13445 (2000).
10. J. Arbiol, J. Cerda, G. Dezanneau, A. Cirera, F. Peiro, A. Cornet, and J. R. Morante, *J. Appl. Phys.*, **92**, 853 (2002).
11. X. Yan, J. He, D. G. Evans, Y. Zhu and X. Duan, *J. Porous Mater.*, **11**, 131 (2004).
12. B. L. Garcia, R. Fuentes and J. W. Weidner, *Electrochem. Solid-State Lett.*, **10**, B108 (2007).
13. K. Cassiers, T. Linssen, M. Mathieu, Y. Q. Bai, H. Y. Zhu, P. Cool and E. F. Vansant, *J. Phys. Chem. B*, **108,** 3713 (2004).
14. C. Bock, C. Paquet, M. Couillard, G. A. Botton and B. R. MacDougall, *J. Am. Chem. Soc.,* **126,** 6026 (2004).
15. D. Liu, Y. M. Lopez-De Jesús, J. Monnier and C. T. Williams, *J. Catal.*, **269**, 376 (2010).
16. E. R. Vance, *J. Am. Ceram. Soc.*, **91**, 3756 (2008).
17. L. Sheppard, T. Bak, J. Nowotny, C. C. Sorrell, S. Kumar, A. R. Gerson, M. C. Barnes, and C. Ball, *Thin Solids Films*, **510,** 119 (2006).
18. K. Kowalski, M. Ijjaali, T. Bak, B. Dupre, J. Nowotny, M. Rekas, and C. C. Sorrell, *J. Phys. Chem. Solids*, **62,** 531 (2001).
19. N. G. Eror, *J. Solid State Chem.*, **38,** 281 (1981).
20. M. H. Wang, R. J. Guo, T. L. Tso and T. P. Perng, *Int. J. Hydrogen Energy,* **20**, 555 (1995).